Color imaging of Mars by the High Resolution Imaging Science Experiment (HiRISE)

W. Alan Delamere [a,*], Livio L. Tornabene [b], Alfred S. McEwen [b], Kris Becker [c], James W. Bergstrom [d], Nathan T. Bridges [e], Eric M. Eliason [b], Dennis Gallagher [f], Kenneth E. Herkenhoff [c], Laszlo Keszthelyi [c], Sarah Mattson [b], Guy K. McArthur [b], Michael T. Mellon [g], Moses Milazzo [c], Patrick S. Russell [h], Nicolas Thomas [h]

[a] Delamere Support Systems, 525 Mapleton Ave., Boulder, CO 80304, United States
[b] Lunar and Planetary Lab., University of Arizona, Tucson, AZ 85721, United States
[c] US Geological Survey, 2255 N. Gemini Drive, Flagstaff, AZ 86001, United States
[d] Ball Aerospace and Technologies Corp., 1600 Commerce St., Boulder, CO 80301, United States
[e] Jet Propulsion Lab., 4800 Oak Grove Dr., Pasadena, CA 91109, United States
[f] CDM Optics, Boulder, CO 80303-7816, United States
[g] University of Colorado, 392 UCB, Boulder, CO 80309, United States
[h] University of Bern, Sidlerstr. 5, CH-3012 Bern, Switzerland

ARTICLE INFO

ABSTRACT

HiRISE has been producing a large number of scientifically useful color products of Mars and other planetary objects. The three broad spectral bands, coupled with the highly sensitive 14 bit detectors and time delay integration, enable detection of subtle color differences. The very high spatial resolution of HiRISE can augment the mineralogic interpretations based on multispectral (THEMIS) and hyperspectral datasets (TES, OMEGA and CRISM) and thereby enable detailed geologic and stratigraphic interpretations at meter scales. In addition to providing some examples of color images and their interpretation, we describe the processing techniques used to produce them and note some of the minor artifacts in the output. We also provide an example of how HiRISE color products can be effectively used to expand mineral and lithologic mapping provided by CRISM data products that are backed by other spectral datasets. The utility of high quality color data for understanding geologic processes on Mars has been one of the major successes of HiRISE.

1. Introduction

The High Resolution Imaging Science Experiment (HiRISE) camera (McEwen et al., 2007a), the most powerful digital imaging system flown beyond Earth's orbit, is carried onboard the Mars Reconnaissance Orbiter (MRO) spacecraft (Zurek and Smrekar, 2007). It has produced a large number of color images of the surface of Mars. In Fig. 1 are examples of the type of false-color images that can be produced with further stretching and intensity enhancement of small areas of the HiRISE images. These images demonstrate the great diversity in the more interesting martian terrains in HiRISE color. Very subtle color differences are seen at the ~1% level. Interpretation of HiRISE color variations has been key to the science results of several papers (e.g., Okubo and McEwen, 2007; McEwen et al., 2007b; Herkenhoff et al., 2007; Grant et al., 2008; Keszthelyi et al., 2008; Weitz et al., 2008; Russell et al., 2008; Geissler et al., 2008). In addition to mapping color units, the data helps resolve the ambiguity between topographic shading and differences in surface mate-

rials. Hence, the 3-color data has proven to be an immense aid to geologic interpretations. The three bands provided by HiRISE are not intended for identifying specific mineral and lithologic surface compositions; however, in conjunction with other multi and hyperspectral datasets (e.g., CRISM), HiRISE color can provide a powerful dataset for detailed photogeologic and mineral/lithologic analysis at sub-meter scales (e.g., Wray et al., 2008).

The camera consists of a 50 cm diameter telescope in front of a focal plane containing 14 Charged Coupled Device detectors (CCDs), each with 128×2048 12 µm imaging pixels, operating as a push-broom system. In September 2006, the MRO spacecraft entered into a mapping Sun-synchronous orbit around Mars, crossing the equator at about 3 PM local mean solar time on the ascending node. The MRO orbital altitude varies from ~250 km over the south polar region to ~320 km over the north polar region. With its one micro-radian per pixel instantaneous field of view (IFOV) and an exposure time of up to 12.8 ms, HiRISE is capable of a ground sampling as small as 0.25 m/pixel at signal-to-noise (SNR) ratios exceeding 100:1, and a swath width of 5.0–6.4 km (20,000 pixels across). The signal from each CCD is output in two separate channels resulting in 28 independent data channels. Each channel is

Fig. 1. Examples of color diversity of the martian surface as seen by the HiRISE camera. All samples are subset false color-infrared from the NOMAP standard products. Scale and further details on these images may be obtained at the HiRISE website using the image IDs shown.

digitized to 14 bit resolution, or 16,384 Digital Number (DN) levels, and the data are stored within the camera electronics. Onboard binning of the data is used in the following modes: 1×1, 2×2, 4×4 pixels (effectively doubling or quadrupling the pixel scale). The BG and IR images usually require 2×2 or 4×4 binning to achieve high SNRs, even when the RED images can be acquired at full resolution. Time delay integration (TDI) allows exposure and SNR control using 128, 64, 32 or 8 lines of signal summation. Non-linear compression to 8 bits followed by lossless data compression may be selected to increase the number of pixels returned by about a factor of 5. This is implemented in the hardware by means of selectable look-up tables that convert the 14 bit data to
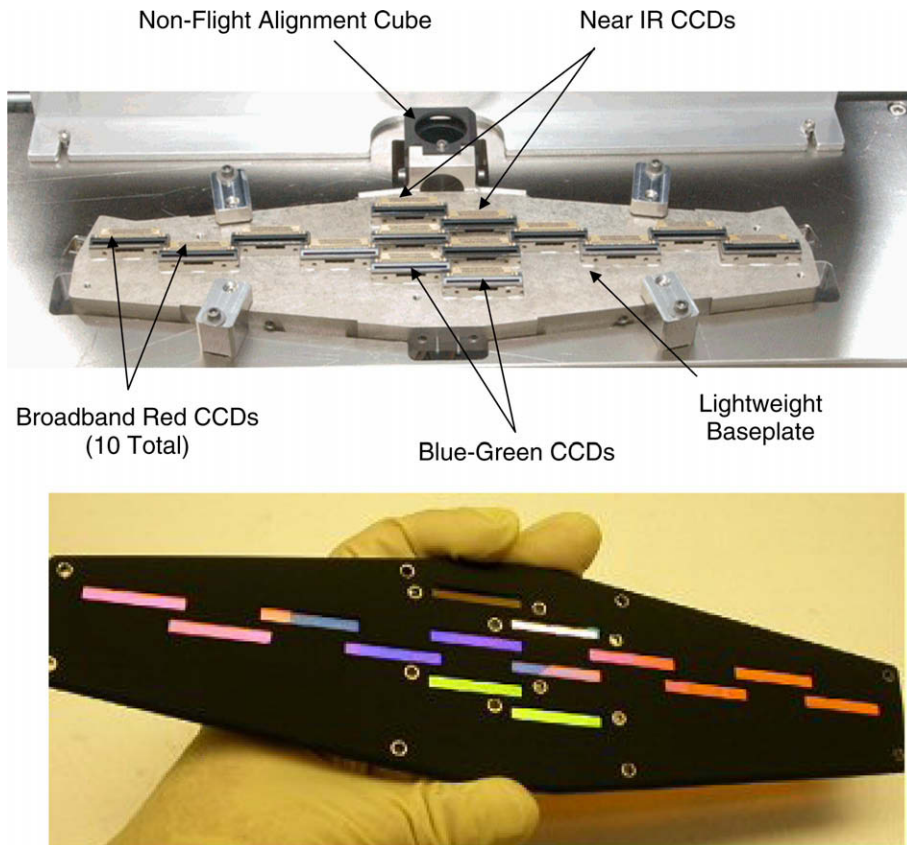
Fig. 2. HiRISE focal plane subsystem components. (Top) The HiRISE focal plane assembly with 14 CCD detectors attached to the base plate. (Bottom) Filter assembly before mounting on the front of the focal plane assembly. Filters are located about 3 cm in front of each CCD.
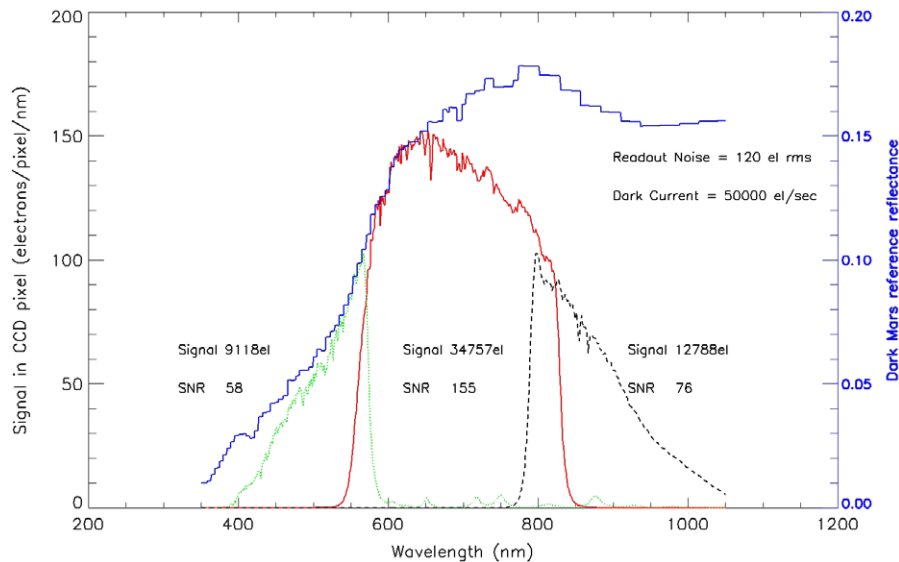

Fig. 3. HiRISE spectral response to a typical Mars dark-region spectrum (blue). The model responses combine the filter, mirror and solar spectrum with the Mars spectrum. The solar incidence angle is 45° and the exposure time is 12.8 ms with 128 lines of TDI.

8 bits, followed by lossless software compression of approximately 2.5×. On the ground the original 14 bit data is recovered. Further details of the experiment and camera design are included in McEwen et al. (2007a, 2009).

Initially, color was not a primary science requirement for the instrument design but was retained throughout the development and fabrication to improve redundancy in the critical central part of the focal plane and to improve measurement of geometric distortions caused by pointing jitter (McEwen et al., 2009). The layout of the focal plane is shown in Fig. 2. The six CCDs in the center are used for color imaging, resulting in HiRISE images with a central swath of color 1.0–1.3 km wide. The 14 CCDs are numbered RED0 through RED9, IR10 and IR11 and BG12 and BG13. The RED CCDs matching the IR and BG CCDs are RED4 and RED5.

The three bandpasses were selected (Fig. 3) to provide the maximum science return, which depends primarily on high resolution and SNR. The full "panchromatic" swath of ten CCDs is acquired through a 550–850 nm bandpass "RED" filter. Observations over this wavelength range reduce the effect of atmospheric hazes seen at shorter wavelengths and capture most of the photons from the generally reddish surface of Mars. The shorter wavelengths are passed through the <600 nm "blue–green" (or BG) filter. The short wavelength falloff of the bandpass is more a function of CCD sensitivity and solar intensity than the filter transmission. This color range was intended to assist in the detection of ice and frost as well as visible spectral slope. The third bandpass transmits >800 nm infrared (IR) light with the long wavelength falloff primarily the result of the CCD response. This region of the spectrum is particularly useful as it is influenced by absorptions arising from iron-bearing minerals. The prediction was that these three bandpasses would allow the differentiation of broad classes of materials (e.g., dust, ice or frost, primary igneous minerals, and alteration products) but specific mineral identifications would require higher spectral resolution (McEwen et al., 2007a). It is important to note that this combination of filters is not optimal for the construction of accurate "true-color" images that match the scene a human eye would see.

Martian color imaging in the visible to near infrared spectral region has been thoroughly reviewed and described in Chapter 8 of *The Martian Surface* (Bell et al., 2008). HiRISE color imaging adds a new dimension to the subject with much higher spatial resolution over selected areas of the surface. We have imaged only ~0.15% of the martian surface in color, yet in pixels of data (1.5 Terra-pixels) it exceeds that of all previous Mars color imaging combined. Much of the color on Mars is dominated by the proportions and distribution of nanophase ferric-oxide bearing dust (red) and ferrous silicate-bearing sand and rocks (e.g., Soderblom, 1992; Bell et al., 2008), the latter appearing more neutral or "blue" in HiRISE false-color images. In general, well-exposed bedrock with more interesting minerals and color diversity has been selected in HiRISE color coverage.

2. Color calibration

Preliminary analysis indicates that the radiometric calibration of processed HiRISE data is generally good to ±20% absolute and approximately 2% relative within an observation. Within a single channel, the pixel-to-pixel radiance values are correct to about 0.5%. However, these values are only approximate because there are continued improvements being made to the radiometric calibration and the analysis of uncertainties is incomplete. In part, this is because of the multitude of different observations acquired for radiometric calibration, including pre-launch images of a calibrated integrating sphere and flight data of the Moon, various stars, Jupiter and its Moons, and Phobos. Augmenting these data are the HiRISE LEDs which illuminate the focal plane with relatively uniform light useful for relative calibration.

The standard Reduced Data Record (RDR) products are delivered with units that can be converted to calibrated I/F by applying multiplicative and additive value to each pixel. This allows quantitative comparison with other data sets. I/F is the calibrated radiance factor, also known as reflectance, defined as the observed brightness relative to the brightness of a Lambert surface illuminated at 0° incidence (i.e., direct illumination) (Hapke, 1981). I is the observed intensity and πF is the solar irradiance at the top of the atmosphere at the time (Mars distance) of the observation through a particular HiRISE spectral bandpass (Danielson et al., 1981). I/F values can be easily compared with similarly calibrated imaging data from other Mars cameras, ground-based observations, and laboratory reflec-

tance spectra. In these units a hypothetical 100%-reflecting Lambertian disk would have an I/F of 1.0 when illuminated normal to its surface.

Each of the three HiRISE color channels is independently scaled to I/F, yielding 3-band color data. These data may be used to help constrain the composition of the martian surface by comparing them with library rock and mineral spectra convolved to the HiRISE bandpasses with the spectral response of each HiRISE color channel. As each channel is radiometrically calibrated, ratios of HiRISE colors are physically meaningful. In contrast, other forms of color enhancement of HiRISE images may not be directly interpretable with respect to martian compositional/photometric variations.

3. Color processing

The five processing steps employed in the production of HiRISE color products are: (1) radiometric calibration and cosmetic corrections, (2) registration of images from each color band using an empirical image correlation technique, (3) increasing the high-frequency detail of BG and IR images using a color-ratio filtering technique, (4) geometric processing and mosaicking of the individual CCDs to form a map-projected product, and (5) converting the images to the JPEG2000 format.

Radiometric calibration, carried out by the ISIS hical program (see http://isis.astrogeology.usgs.gov), corrects for instrument dark current and offset, and variable detector gain, then converts the data to I/F. After hical one typically sees up to a 1–2% brightness mismatch between the two channels of a CCD and among the CCDs that comprise the observation. This mismatch is due to instrument behavior that has proven difficult to model, and is normalized by applying multiplicative values to force the averages to be the same at the channel join and CCD overlap areas. Because the data from CCD/channel IR10_1 (and IR10_0 to a lesser extent) is especially prone to bit-flip errors (McEwen et al., 2009), it is often not included in the color products. Because IR10 images typically contain bit flips a noise reduction filter is applied to these data to replace these erroneous pixel values with the average of surrounding valid pixel values. Sometimes pixel-scale shadows are erroneously replaced, although reprocessing planned for early 2009 should eliminate this artifact.

Spacecraft pointing jitter (McEwen et al., 2009) requires that we spatially co-register the image data for the color CCDs. The CCDs see the same point on the surface at different times separated typically by about 120 ms (each color CCD is spaced on the focal plane about 1200 lines apart in the direction along the orbit ground track). In this time interval, the spacecraft jitter can cause unpredictable translation errors up to tens of pixels in magnitude. In the color co-registration process, the IR10-RED4-BG12 and IR11-RED5-BG13 color sets are processed separately.

The first step in the co-registration process converts the binned IR and BG CCD image data to match the binning of the RED CCD. The IR and BG images are expanded using bilinear interpolation. The IR and BG images are usually acquired in bin 2 or 4 mode while the RED images are typically acquired in bin 1, but can also be acquired in the bin 2 or 4 mode. The higher binning of IR and BG imaging helps minimize the downlink volume and also provides a higher SNR for these bands. In a subsequent step, described below, the high-frequency spatial content of the RED imaging, with higher SNR for the bin 1 imaging, is added to the IR and BG imaging providing a sharper color image product.

In the next step, an ISIS program (*hijitreg*) builds a control grid that spatially maps the IR and BG pixels to their corresponding RED pixels. The control grid is derived by correlating the local image data at each grid intersection. In the final step, the ISIS program known as *slither* uses the control grid pixel mapping from *hijitreg*

to geometrically warp the IR and BG image data to spatially match the RED. Although this procedure generally works well, the algorithm occasionally fails to produce well-registered images, especially when the SNR of surface features is poor due to atmospheric conditions. However, in most cases the observations are well registered and released to the PDS without further attempts to improve the registration.

A simple spatial-enhancement technique is applied to some of the IR and BG images after they have been scaled and co-registered to match the RED. Recall that the IR and BG images typically have a larger pixel scale because they are consistently acquired with a higher binning mode (e.g., Bin 1a would refer to all red channels in bin 1 mode with IR and BG taken in bin 2 mode. See Table 2 for other examples). The high-frequency detail of the RED image is propagated to the IR and BG images by a ratio and filtering process. First, IR/RED and BG/RED ratio images are created. For bin 2 color images, a 3×3 boxcar lowpass filter (5×5 for bin 4) is applied to the ratio images. The filtered ratio images are then multiplied by the original RED image to restore the IR and BG images but spatially enhanced with the RED image high-frequency content. The filtering on the ratio also has the added benefit of interpolating any rejected pixels that were previously identified as noise. However, a science user interested in interpreting color variations at the scale of individual pixels (which we do not recommend) should first reprocess the images without the spatial-enhancement processing.

In the geometry processing step, the IR10-RED4-BG12 and IR11-RED5-BG13 color sets are individually map projected (ISIS program *cam2map*) then mosaicked together (ISIS program *himos*) to form a single image of the two color sets. Observations in the latitude range $-65°$ to $65°$ are mapped to the Equirectangular Projection; the higher latitudes are mapped to the Polar Stereographic projection. The map products are uniformly scaled to 0.25 m/pixel for bin 1 observations (0.5 m/pixel for bin 2 and 1.0 m/pixel for bin 4).

3.1. Reduced-data-record color products

The archive of radiometrically-corrected map-projected color products (RDRs) are permanently stored and disseminated by NASA's Planetary Data System (PDS) Imaging Node through its HiRISE Data Node located at the University of Arizona. During active mission operations new products are released every three months, in addition to a set of five to ten images released weekly with captions on the HiRISE website throughout the Primary Science Phase.

In the final data preparation step, the RDR color products are converted to the JPEG2000 format accompanied by a detached PDS label. The companion PDS label is contained in a file of the same name but with extension LBL. The PDS label contains useful information about the observation, including how to convert the integer pixel values to *I/F*, map projection information, and instrument commanding that was used to acquire the observation. Color products are made available through the HiRISE web site (http://hirise.lpl.arizona.edu), the PDS online archive volume (http://hirise-pds.lpl.arizona.edu/PDS/), the PDS Imaging Node (http://pds-imaging.jpl.nasa.gov/), and the PDS Geosciences Node (http://pds-geosciences.wustl.edu/). Useful tools and freeware, for accessing and displaying images stored in the JPEG2000 format, are described at the HiRISE web site (http://hirise.lpl arizona.edu/tools/ and http://hirise.lpl.arizona.edu/HiBlog/?tag=expressview).

A color RDR product is stored as a false-color 3-band image (band 1 = IR, band 2 = RED, band 3 = BG) with 10-bit pixels (1024 DN levels). The calibrated *I/F* pixel values are normalized to the 10-bit integer values by identifying a minimum and maximum *I/F* value in the three-band image then linearly mapping the minimum to 0 and the maximum to 1023. There are two keywords in the PDS label that provide a mechanism for converting the integer pixels back to *I/F*. The SCALING_FACTOR and OFFSET keyword val-

Table 1
Available image products.

Format/file name extension	Description
_IRB.NOMAP.JP2	Enhanced false-color image (band 1 = IR, band 2 = RED, band 3 = BG). Image maintains the original spacecraft viewing geometry. Each color band is independently stretched to maximum color contrast. Images are slightly lossy compressed to reduce the data product size
_RGB.NOMAP.JP2	Enhanced 3-color image consisting of the RED (band 1), BG (band 2), and "synthetic blue" (band 3). Image maintains the original spacecraft viewing geometry. Each color band is individually stretched to maximum color contrast. Images are slightly lossy compressed to reduce the data product size
_COLOR.QLOOK.JP2	Map-projected enhanced false-color product similar to the RDR color products but with the color bands (band 1 = IR, band 2 = RED, band 3 = BG) independently contrast stretched to maximize color contrast. Images are slightly lossy compressed to reduce the data product size
.browse.jpg	Reduced-scale jpeg images used for browsing through the image collection. There is a browse jpeg file for each color product
.thumb.jpb	Highly reduced-scale jpeg image intended for web applications that need thumbnail images. There is a thumbnail jpeg image for each color product

ues in the IMAGE object are used in the conversion: $I/F = (\text{PIXEL\_VALUE} * \text{SCALING\_FACTOR}) + \text{OFFSET}$.

The color RDR products exist as individual files with the naming convention XXX_YYYYYY_ZZZZ_COLOR.JP2 (example: PSP_001333_2485_COLOR.JP2, for more information, see http://hirise.lpl.arizona.edu/HiBlog/?tag = observation-id), where XXX is the mission phase (e.g., TRA, PSP, ESP, etc.), YYYYYY is the orbit number, and ZZZZ is the latitude/node target code (e.g., on the ascending node: 0900 = 90° S, 1800 = 0°, 2700 = 90° N). The color RDR products can be directly accessed on the PDS archive volume located at the HiRISE Data Node (http://hirise-pds.lpl.arizona.edu/PDS/RDR/).

3.2. Color "extras" products

The official PDS products are enormous files, typically larger than 1 GB in size, and can be difficult to work with. So we have created RDR "Extras" products at reduced scale or with slightly "lossy" compression to produce smaller files that are much easier to display. "Lossy" compression eliminates some small-scale detail (mostly random noise), enabling compression into smaller files that are easier to transfer, store, and manipulate. Additionally, the contrast of each individual color band is independently stretched in order to maximize the color contrast of the observation. However, with these color-enhanced images it is not possible to restore calibrated *I/F* values to carry out quantitative work (use the formal RDR products for quantitative work). There are two types of color Extras products available: un-projected products that maintain their spacecraft viewing geometry ("QLOOK"), and the map-projected products like the RDR products. Additionally, there are reduced-resolution JPEG products used for browsing the image collection. Table 1 summarizes the color "Extras" products.

Those that wish to process the HiRISE data for themselves can use the Integrated Software for Imagers and Spectrometers, version 3 (ISIS3) as described above. The three-color products are illustrated in Fig. 4. The "IRB" products use the full spectral range of HiRISE. The "RGB" product uses the RED in the red and BG in the green channels, respectively, and uses a synthetic blue image. The synthetic blue image DNs consist of the BG image DN multiplied by 2 minus 30% of the RED image DN for each pixel. This is
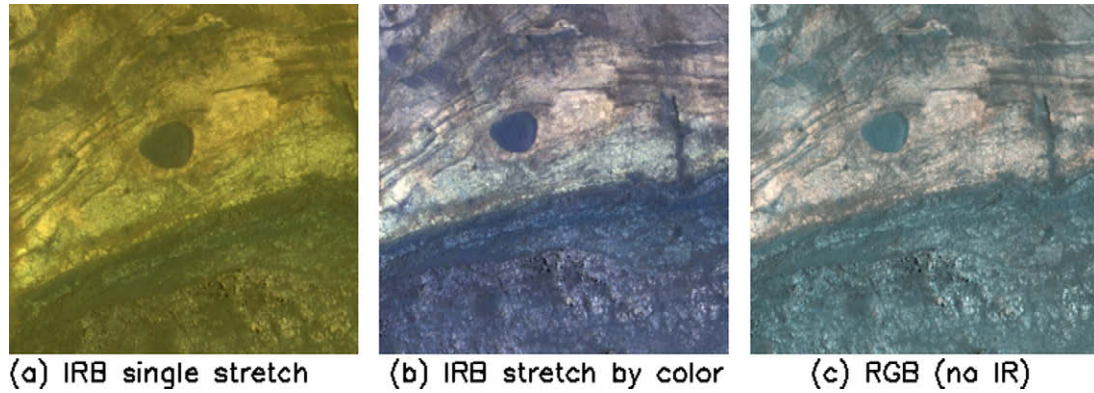
(a) IRB single stretch **(b) IRB stretch by color** **(c) RGB (no IR)**

Fig. 4. Shows color products for observation PSP_002176_2025, 280 m by 280 m. The color RDR products (a) are made up of the IR (red channel), RED (green channel), and BG (blue channel) filters with each band identically stretched. The PDS labels that accompany the RDR products contain information on how to translate the pixel integer values to I/F. Each color band is stretched independently for the "NOMAP" products (b and c). The IRB products (b) use the IR (red channel), RED (green channel), and BG (blue channel) filers. The RGB products (c) use the RED (red channel), BG (green channel), and a synthetic blue (blue channel) filters. The RGB products transfer the often-dominant RED–BG differences to the warmer colors. In this figure the RDR map-projected product was rotated to match the orientation of the NOMAP products.

not unique data but provides a more appealing way to display the color variations across a 3-color channel system when just two bandpasses are available. The algorithm attempts to broadly extrapolate what a blue part of the spectrum might look like but the RGB product should not be thought of as a "true color" image because each band, including the synthetic blue, is individually stretched. The particular formula has the advantages of being simple and it avoids creating negative numbers in the output file. The RGB image is useful when IR10_1 is not processed and to transfer the often-dominant RED–BG differences to the warmer colors.

All stretched products used a dark area of the image as the zero reference. This is determined by binning the image by 9×9 and finding the minimum value. The minimum (offset) is subtracted from the image. The image is then stretched to cover the 10-bit range of the image storage system. The use of 10-bit pixels allows for the expanded dynamic range when companding the non-linear look-up tables (LUTs) used on the HiRISE instrument to convert from 14-bit to 8-bit pixels.

4. Observational optimization

4.1. Exposure determination for observations

The first step in the acquisition of a color HiRISE image is the generation of the appropriate commands. As described in McEwen et al. (2007a, 2007b), there are hundreds of different modes in which a HiRISE image can be acquired. However, in practice we have used only a few of these modes. The key settings that must be selected are (a) binning mode where the selection is between values of 1, 2, or 4 (b) TDI level where the selection is between the values of 128, 64, 32, or (very rarely) 8 and (c) LUT compression where the selection is among 28 custom designed look-up tables. Higher bin modes reduce the spatial scale of a pixel but increase the signal by summing 4 or 16 pixels (in BIN2 or BIN4 mode, respectively). TDI affects the signal level by controlling the number of pixels summed before the signal is read out from the detector. The LUTs are for the onboard conversion of the data from 14 to 8 bits per pixel. Conversion to 8 bits enables the lossless onboard compression to be used resulting in an average of about 3.2 bits per pixel for storage and transmission. See further details in McEwen et al. (2009).

HiRISE exposure control uses a camera model and the expected Mars albedo and lighting to optimize the exposure to achieve the highest signal-to-noise ratio. The exposures are adjusted by select-

Table 2
Typical imaging parameters.

Image	Red		NIR		BG	
	TDI	BIN	TDI	BIN	TDI	BIN
PSP 005778 2140	128	1	32	4	32	4
PSP 004004 0670	128	1	64	4	64	4
PSP 004010 1500	128	1	32	4	64	4
PSP 004097 2185	128	1	128	2	128	2
PSP 005302 0880	128	2	64	4	128	4

ing the number of TDI lines and the binning factor for each color filter independently. Examples of typical imaging parameters are illustrated in Table 2. Bin 1 TDI 128 is normal for the red filtered CCDs at mid to low latitudes when the data rate is high. The signal is significantly lower with the IR and BG filtered CCDs so bin 2 or 4 is used. Bin number changes signal levels by approximately factors of 4 and 16 as we go from 1 to 2 to 4. TDI is the fine control reducing exposure by factors of 2, 4, and 16 as we go from 128 to 64 to 32 to 8. TDI = 8 is rarely used. Higher bin numbers are used when the spacecraft data rate is low to maximize coverage.

4.2. Contrast in color images

Mars is relatively bland in the bandpasses selected for HiRISE color. This is in large part due to the dusty atmosphere, but also to surface dust cover as well as coatings and other unremarkable surface deposits. This blandness generally translates into limited contrast in remote sensing images acquired in the visible wavelengths. However, the large dynamic range, high spatial resolution and SNR of the HiRISE detector allow even subtle variations in the surface colors to be recorded. The non-linear LUTs used to compress the 14 bit data to 8 bits preserve most of the information captured by the detector. Fig. 5 right shows histograms of an observation of Victoria Crater, which was recently explored by the Opportunity rover (Squyres and Arvidson, 2008), that was taken with no LUT applied so that all 14 bits in each pixel were preserved. Fig. 5 left shows histograms for a region in Ismenius Lacus. The red channel was acquired in 14 bit mode to preserve the highest quality data while the IR and BG channels used 4×4 binning. The signal has three components, solar reflection from atmospheric dust & aerosols, sky light illumination of the surface and solar illumination of the surface. In the HiRISE images the latter is only
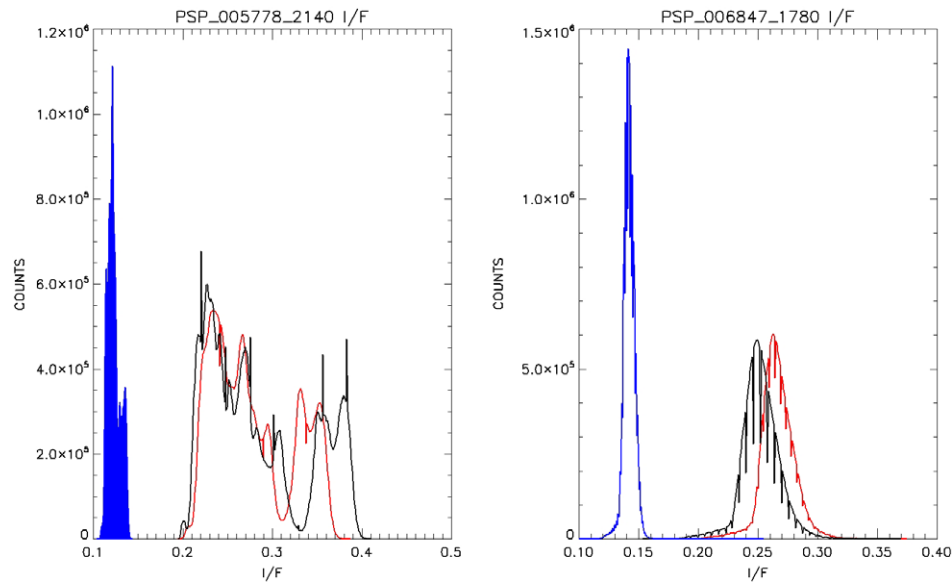
Fig. 5. Histograms of Victoria Crater image (PSP_006847_1780) and Ismenius Lacus (PSP_005778_2140) for the three color channels, red is the RED channel, black is the IR channel and blue is the BG channel. Note that the RED and IR are similar in *I/F* units while the BG is significantly lower.

40 to 55% of the total signal as can be seen in the narrow histograms of *I/F* (Fig. 5, right). These histograms illustrate the dynamic range, sensitivity, and overall quality of the HiRISE camera for imaging "bland" martian scenes. With such capabilities HiRISE can be used, in conjunction with CRISM or other spectral datasets, to locate fine scale variability in mineralogy across the martian surfaces. This is further explored (by example) in a following section.

5. What do the colors in HiRISE PDS-released images mean?

In spite of the variable level of color enhancement for the Extras products (described above), we can make some generalizations to better understand what the stretched color images are showing. Dust (or indurated dust) is generally the reddest material present and looks reddish in the RGB color and yellow in the IRB color products. Coarser-grained materials (sand and rocks) are generally bluer (or sometimes cyan to violet in IRB color) but also relatively dark, except where coated by dust. Frost and ice are also relatively blue–white, but very bright, and are spatially concentrated at the poles or on pole-facing slopes and varies with the seasons. Some bedrock is also relatively bright and blue, but not as much as frost or ice, and rock and ice are morphologically distinct from one another. The IR and RED bandpasses are often highly correlated so the IR provides little new information, and the RGB color does a better job of showing the RED vs. BG color variations by moving these differences into the warmer colors. Also, because one of the four IR channels is often problematic, it may be excluded from the RDR products. The RGB color usually covers the full color swath, because it uses only the RED and BG channels. The IR channels do provide unique information in some small but important areas on Mars. For example, mafic minerals (e.g., olivine, pyroxene, or calcic plagioclase feldspar) or a diversity of hydrated minerals (e.g., phyllosilicates) stand out in the 3-color data. The best way to understand what the HiRISE colors indicate about composition is to compare them directly to products derived from the ~18 m/pixel CRISM data (Murchie et al., 2007, see http://crism.jhuapl.edu/).

Another benefit of the color is that it helps resolve ambiguities in grayscale images. One region may be brighter or darker than an-other due to different materials on the surface, different slopes and angles of illumination, or differences in atmospheric haze, and it can be difficult to distinguish these contributions by examining a grayscale image. With the color images this ambiguity is resolved because different materials have different colors while the shadowed areas are dark in all colors. Stereo images and topographic data provide an alternate means of resolving this ambiguity.

5.1. Color artifacts

There are several artifacts that can be found in HiRISE color products. Here, we describe the most common artifacts observed and their source. Common artifacts in HiRISE color can arise from misregistration, spurious colored pixels in very low-DN or very high-DN (potentially saturated) areas when stretched, cosmic-ray hits during image acquisition, calibration issues, missing data and various sources of noise. Misregistration of HiRISE color bands, is often manifested as parallel bands of intense colors near bright-dark edges (e.g., outline of a boulder or outcrop). Properly registered HiRISE color can also give this appearance, but with more muted colors, and is often due to asymmetric distribution of dust over the topography. Another artifact is the variability of color within shadows. Shadowed areas may possess different colors (as on Earth), but can be exaggerated by the automatic contrast stretches. This automatic contrast stretching can also create unusual colors (actually more realistic colors) in frost/ice-free surfaces in a scene where some bright frost or ice is present, as these bright patches control high DN stretch values in all three channels. Another artifact in HiRISE color images is erroneous colors near the center of each set of CCDs, or near samples 1000 and 3000 in unbinned NOMAP images (columns 500 and 1500 in 2 × 2 binned images). This is due to "furrows", a calibration issue in the center columns where the data are split and read out into the two channels. Also, some of the early HiRISE images included saturated pixels due to the choice of LUTs. If the very brightest highlights have strange colors, this could be due to pixel saturation. Sometimes small bright spots, lines, or jagged patterns are observed in one of the color channels and are most likely the result of cosmic-ray hits during image acquisition. Rectangular patterns with very bright colors due to zeros in one or more channel are caused by

loss of data telemetry from MRO to the ground stations. Images obscured by atmospheric dust, haze or clouds generally appear noisy. However, in some cases the air is clear and the surface is particularly bland, so stretching the image to enhance the surface features will also enhance the noise. Condensate hazes and clouds can create diffuse color variability that does not correspond to the distribution of surface materials (McCord et al., 2007). This is especially obvious in the BG, and can sometimes be observed in corresponding MARCI images. Several of the channels have noise or DN dropouts due to bit flips when the electronics have cooled down between image acquisitions, this is particularly apparent in both channels of CCD IR10. These bad data sometimes lead to poor contrast stretches and odd colored pixels. One other CCD, BG13, very rarely suffers from a malfunction that creates down-column smear. Early during PSP, we applied more pixel binning (4 × 4 rather than 2 × 2) to BG13 than to BG12, resulting in loss of color resolution over half of the color image.

The examples of two artifacts are shown in Fig. 6 are extreme cases. In Fig. 6A the problem is caused by the gain changing as the electronics warms up. (To minimize power consumption the CCD electronics are turned off between images.) Each CCD channel has slightly different warm-up time constants resulting in different rates of change of gain. This effect has been reduced by increasing the warm-up time and improving the calibration software. The second example, Fig. 6B, illustrates the importance of the high stability operational mode. In this extreme case a HiRISE observation was taken while the spacecraft was being disturbed (usually from movement of other instruments or the solar arrays).

In general, these color artifacts are very subtle and the user should examine and understand the raw data before claiming discovery of something unusual on Mars.

6. Band ratios

We have been experimenting with a band ratio composite of the color channels to standardize the information contained therein regarding the potential mineral and lithologic composition of the martian surface. CRISM was particularly designed to detect electronic transitions in Fe-bearing minerals in addition to their alteration products, and vibrational absorptions due to the presence of H_2O, OH, CO_3, and SO_4 bearing species in surface materials at a spatial resolution of ~18 m/pixel (Mustard et al., 2008). We can use the color information from HiRISE to assess sub-pixel mixing of the CRISM spectral data. There are a large number (5184 in Bin 1) of HiRISE pixels in one full-resolution CRISM pixel (~18 m/pixel). It would be valuable to know the potential spectral variability within a CRISM pixel. To begin, we processed visible–infrared mineral spectra from the USGS spectral library (Table 3; Clark et al., 1993) through the HiRISE radiometric model. Fig. 7 shows the results of this study. Primary mafic minerals and lithologic materials (e.g., 1 Dunite) are tightly clustered with respect to IR/BG and BG/RED values. This is a consequence of the predominance of ferrous vs. ferric iron in these geologic materials (e.g., Pieters and Englert, 1993). Secondary and alteration minerals often possess larger contributions of ferric over ferrous iron, which effectively increase IR/BG and IR/RED while lowering BG/RED (e.g., Pieters and Englert, 1993; Vincent, 1997). Essentially, HiRISE color can aid in the identification of unaltered and altered Fe-bearing materials due to the sensitivity of the HiRISE bandpasses to ferrous vs. ferric absorptions in the VNIR wavelength region. However, we must emphasize that HiRISE color alone cannot be used to map specific mineral-rich units without the aid of a multispectral or hyperspectral dataset such as CRISM, OMEGA, THEMIS, or TES.

Fig. 7 plots show that the HiRISE data may be useful in distinguishing ferric vs. ferrous iron-bearing minerals and assessing the sub-pixel distribution of materials identified using CRISM and other spectral datasets. We illustrate a band ratio composite from a HiRISE image covering a well-documented olivine- and phyllosilicate-rich area; the grayscale images are shown in Fig. 8. To get a feel for the I/F band ratio values in the above images all the data points are plotted in Fig. 9. Histograms of the band ratios are shown in Fig. 10. In Fig. 11 the band-ratio images are shown.

To visualize the mineral variability a false-color band ratio composite is shown in Fig. 12. It consists of IR/RED ratio in the red channel, IR/BG ratio in the green channel, and BG/RED ratio in
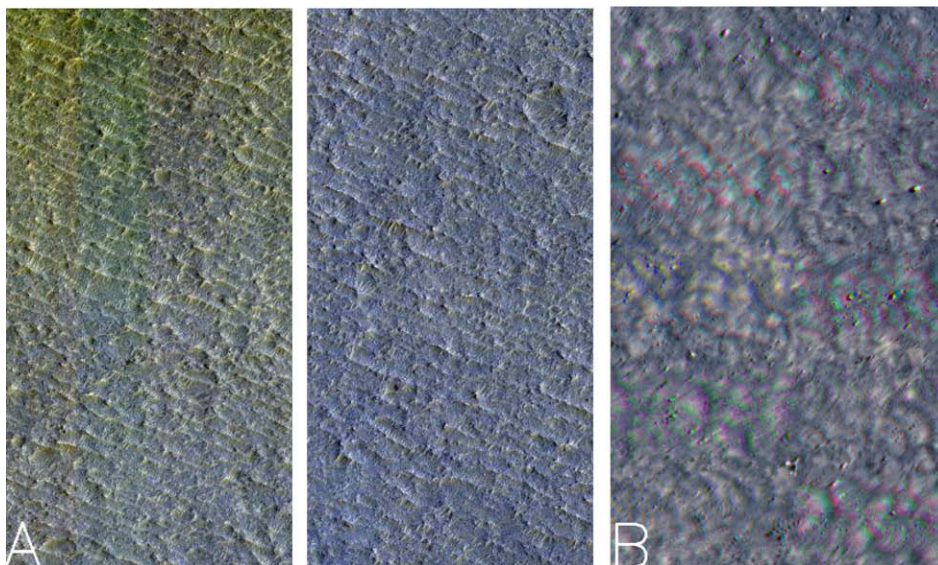

Fig. 6. Artifact examples. (A) Observations with low color contrast can exhibit an artificial color shift at the beginning of an image. In this example the image is artificially yellow at the top for the first thousand lines and neutral for the next thousand lines. These color shifts are a result of instrument gain drift that has not been completely corrected. Gain changes at different rates for each color channel. Recent processing changes have significantly reduced this effect. (B) Improper operation of the spacecraft can cause smear, degrading the resolution and causing color errors in this example. Color anaglyph glasses can be used to see spacecraft wave motion. This image is 600 by 1000 lines at the join of two CCDs. The adjacent CCD images are separated in time by about 60 ms.

Table 3
Laboratory mineral spectra used in study. See Fig. 8.

Ferrous		Ferric	
Number	Laboratory mineral	Number	Laboratory mineral
0	Diopside	2	Ferrihydrite
1	Dunite	3	Iron-substituted montmorillonite clay
7	Hypersthene	4	alpha-FeOOH, goethite powder
10	Muscovite	5	alpha-Fe_2O_3, hematite powder
13	Olivine	6	Mauna Kea Palagonite HWMK20
16	Anorthite GDS28 Syn <74 μm	8	Jarosite industrial lag deposit
17	Augite NMNH120049	9	Jarosite NMNH95074–1
18	Labradorite HS17.3B	11	Nanophase alpha-Fe_2O_3, hematite powder
19	Olivine GDS71.b Fo91 <60 μm	12	Nontronite, Fe-rich smectite clay
20	Olivine KI3054 <60 μm Fo66	14	Nanophase hematite
21	Olivine KI3188 <60 μm Fo51	15	gamma-Fe_2O_3, powder
22	Olivine KI4143 <60 μm Fo41	24	GRL bright BellMustard
23	Pigeonite HS199.3B	25	Mars albedo_bright
		26	Mars dark
		27	Ophir bright region composite spectrum

the blue channel. All are byte scaled to the boxes shown in Fig. 9. This is a full resolution image of 1000 by 1000 pixels with 28 cm/pixel scale. (Approximately 15 by 15 CRISM pixels cover this area) The IR & BG data are bin 2 (500 × 500 pixels) re-scaled to 1000 × 1000. The use of band ratios has removed most of the topographic shading so the color must relate to mineral characteristics. In general, the blue color represents ferrous bearing minerals and the yellow ferric bearing. Identification of minerals by color in this image may be possible to a limited extent but the real value is in extending the CRISM results to smaller scales.

6.1. Comparison with CRISM data

Mineral and lithologic mapping may be extended from kilometers down to meter scales by using HiRISE color information in conjunction with the acquired multispectral (e.g., THEMIS) and hyperspectral (e.g., TES, OMEGA and CRISM) datasets for Mars. As an example, we have chosen a well studied and characterized location within the region surrounding the Nili Fossae (Fig. 13). This spectrally diverse area of Mars has been mapped in detail using previously available orbital spectral and visible datasets, and has become well known for both its mafic (Hamilton et al., 2003; Hoefen et al., 2003; Hamilton and Christensen, 2005; Tornabene et al., 2008) and hydrated silicate mineral diversity (Mangold et al.,
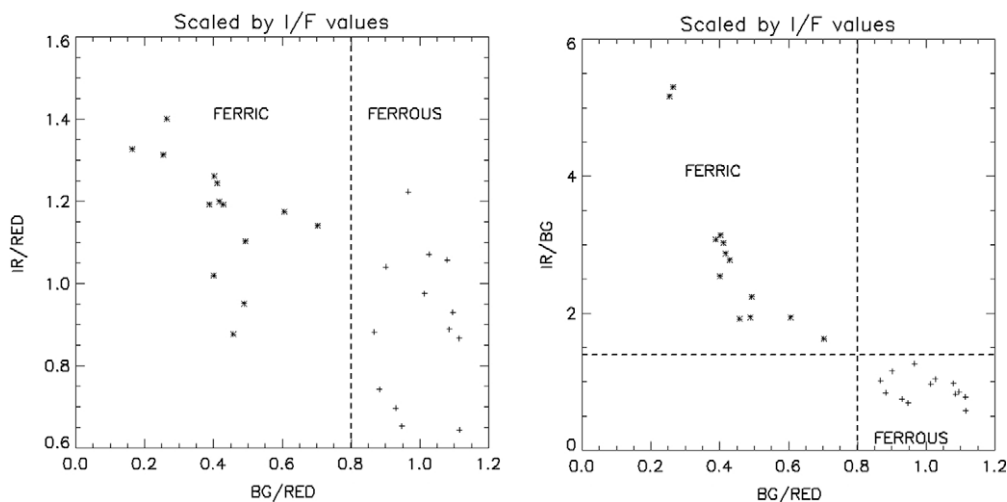

Fig. 7. Band ratio values derived from laboratory mineral, lithologic and surface spectra weighted by the HiRISE spectral response. The minerals chosen for this plot were selected based on their detection from other Mars spectral datasets, or their presence in martian meteorites. We do not claim to be able to distinguish the individual phases plotted here. The three HiRISE bandpasses are particularly sensitive to ferrous vs. ferric iron contents in these minerals, which can be seen here (see text for more information). The mineral, lithologic and surface spectra used are shown in Table 3.

Fig. 8. PSP_002176_2025. Selected 1000 × 1000 area from CCD channels 5-1, 11-1, and 13-1. The image area is 282.5 m by 282.5 m.

2007; Mustard et al., 2007, 2008). A synthesis of these studies indicates the presence of basaltic materials both rich and poor in olivine, hydrous silicate-bearing materials, and terrains rich in the low Ca variety of pyroxene (e.g., enstatite, pigeonite, etc.). Here we compare and contrast a coordinated CRISM Full-Resolution Targeted (FRT) observation with the color-infrared and band ratio color products derived from its corresponding HiRISE image (PSP_002176_2025) centered on 77.06° E, 22.26° N in the vicinity of the Nili Fossae.

The CRISM RGB composite in Fig. 14A consists of a radiometerically and atmospherically corrected summary product using the multi and hyperspectral band parameters defined by Pelkey et al. (2007) and the CRISM science team (Ehlmann, B., 2008, personal communication). Band parameters OLINDEX, D2300 and BD1900R were chosen to highlight the presence of olivine and hydrous silicates (including Fe–Mg phyllosilicate-bearing materials) and create a color-composite image (Fig. 14A). The OLINDEX, used in the red channel, specifically takes advantage of the broad ∼1.0 μm feature due to the presence of ferrous iron-bearing component (or the fayalitic solid-solution end member) of olivine. The D2300 and BD1900R parameters were used in the green and blue channels, respectively, and were chosen to highlight the presence of Fe–Mg-
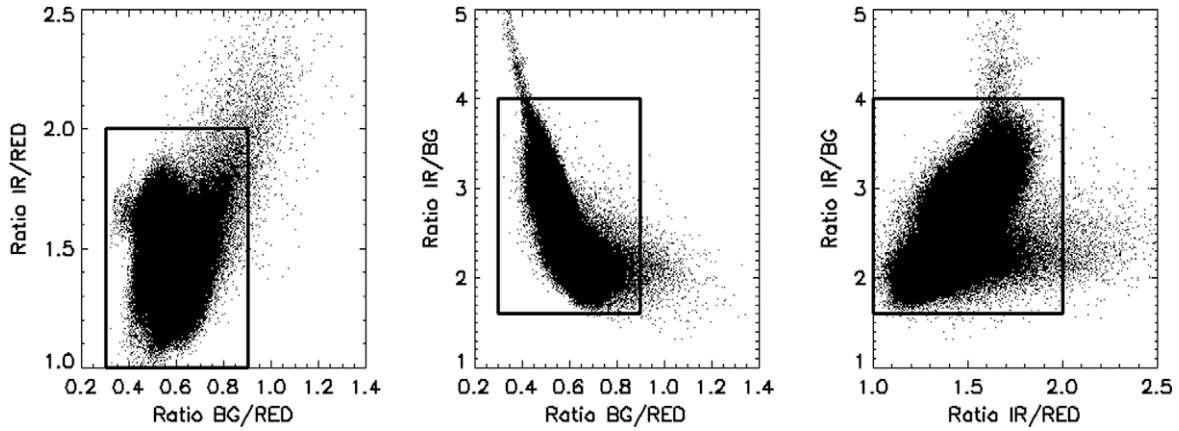

Fig. 9. Plots of all data points in the 1000 × 1000 subset from the HiRISE ratios from image PSP_002176_2025. The boxes are arbitrary limits for producing a color stretch for these images.
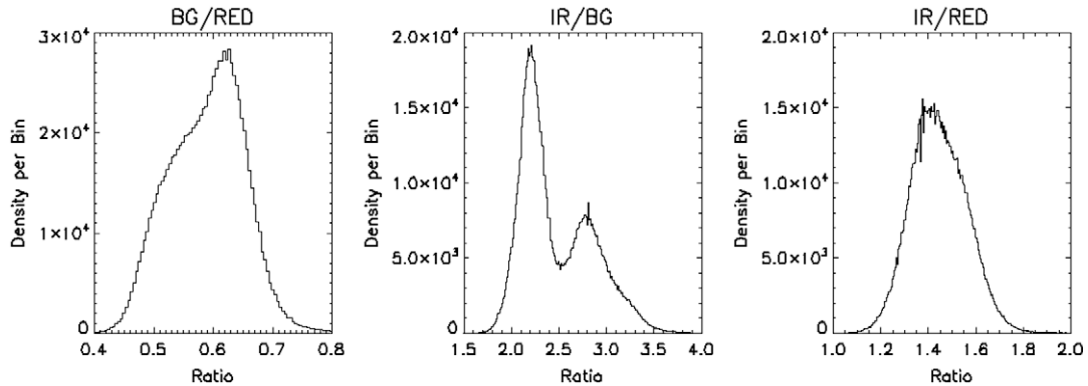

Fig. 10. Histograms for the 1000 × 1000 subset from the HiRISE ratios from image PSP_002176_2025. The bin number is the ratio value.
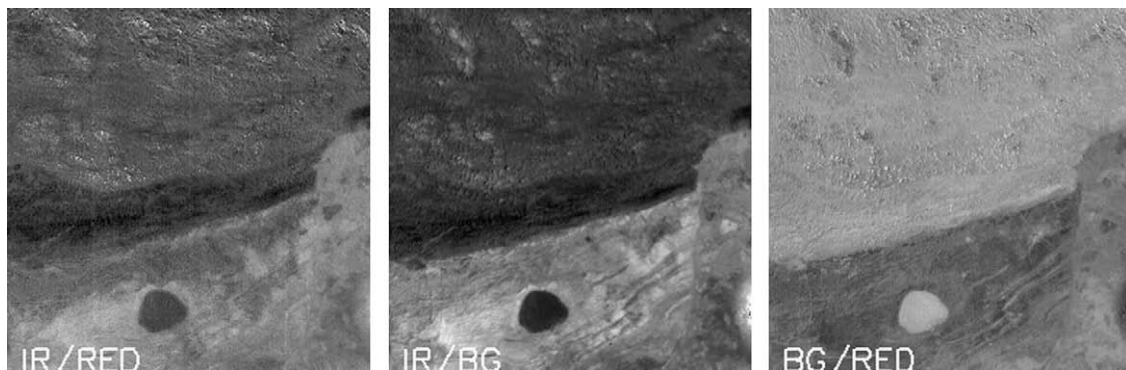

Fig. 11. Ratio of I/F values of the three images. All three images are byte scaled with the limits (boxes) shown in Fig. 9.
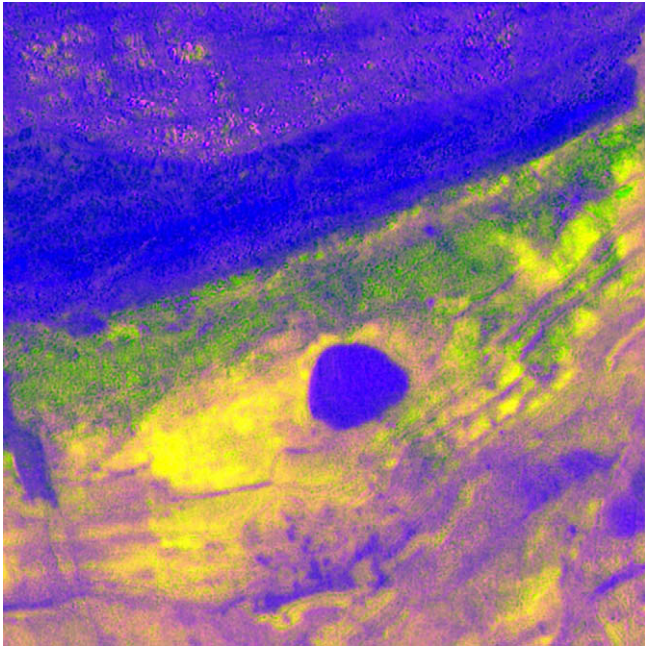
Fig. 12. HiRISE color band-ratio image consisting of the IR/RED ratio in the red channel, IR/BG ratio in the green channel, and BG/RED ratio in the blue channel. All are byte scaled to the boxes shown in Fig. 9. This is a full resolution sub-image of 1000 by 1000 pixels with 28 cm/pixel resolution. (Approximately 15 by 15 CRISM pixels cover this area.)

rich phyllosilicates (∼2.3 μm feature) bearing an interlayer water molecule (∼1.9 μm feature) in cyan with green areas possessing a weak or absent ∼1.9 μm feature and blue areas possessing a weak or absent ∼2.3 μm feature. In order to facilitate a comparison between the HiRISE color products and the CRISM band parameter color composite, we have overlain the color information from CRISM on the HiRISE red mosaic product using a Hue, Saturation and Value (HSV) color transform algorithm (Fig. 14B). HSV transforms an RGB image (i.e., CRISM) to HSV color space, then replaces the value band (typically a grayscale high-resolution image – the HiRISE red mosaic image – which supplies only intensity to the color inputs), and automatically re-samples hue and saturation to the high-resolution pixel size using a nearest neighbor technique; the final step then places the image back into RGB color space (e.g., Gillespe et al., 1986). The output RGB image will have the same pixel scale of the input high-resolution data (i.e., HiRISE red mosaic). Our resultant HSV color transformed product shows that the CRISM color-coded composition correlates quite well with morphological features and albedo variations in the HiRISE red mosaic image (e.g., bedrock, stratigraphy, craters and dune forms, etc.) The standard HiRISE infrared color product (Fig. 15A), but in particular a color composite consisting of band ratios (Fig. 15B), correlates well with the compositional units defined above and as shown in a close-up of the HSV transformed HiRISE-CRISM product in Fig. 15C.

Table 4 summarizes the correlations between the two HiRISE color products and the HSV transformed HiRISE-CRISM image composite. In general, darker colors (blue) within the ratio image are more consistent with surfaces dominated by ferrous minerals
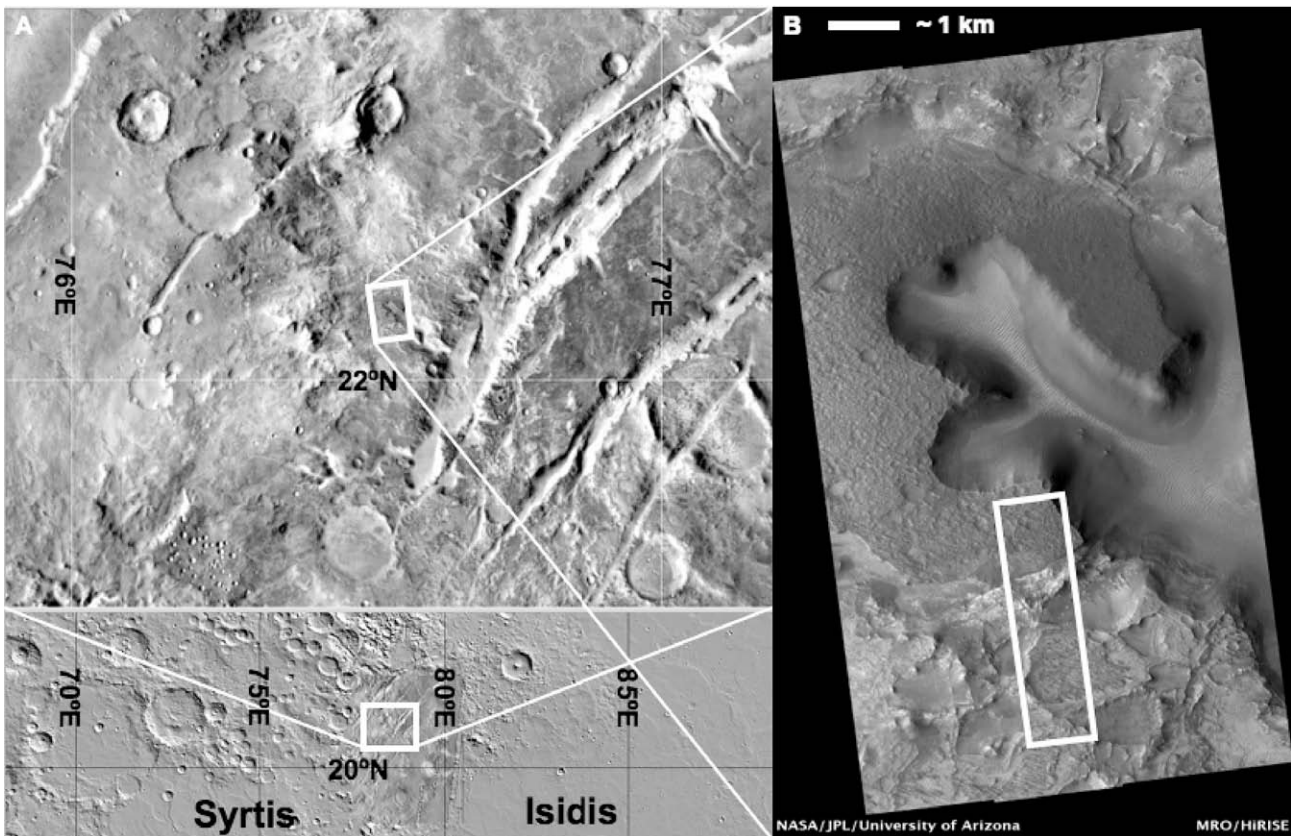

Fig. 13. Context images providing the location and both regional and local geomorphology of the area selected for CRISM/HiRISE comparison. This location highlights a ∼6-km diameter unnamed crater that reveals stratigraphy and embayment relationships with spectrally diverse geologic materials in the vicinity of the Nili Fossae troughs. (A) Local and regional views of the location of the coordinated HiRISE and CRISM images using the full resolution THEMIS daytime IR mosaic (above and below) and the MOLA shaded relief map (below). Views courtesy of JMARS GIS software (Weiss-Malik et al., 2005). (B) HiRISE red mosaic browse product (PSP_002176_2025) centered at 77.06°E, 22.26°N and corresponding to the central portion of the CRISM image shown in Fig. 14.
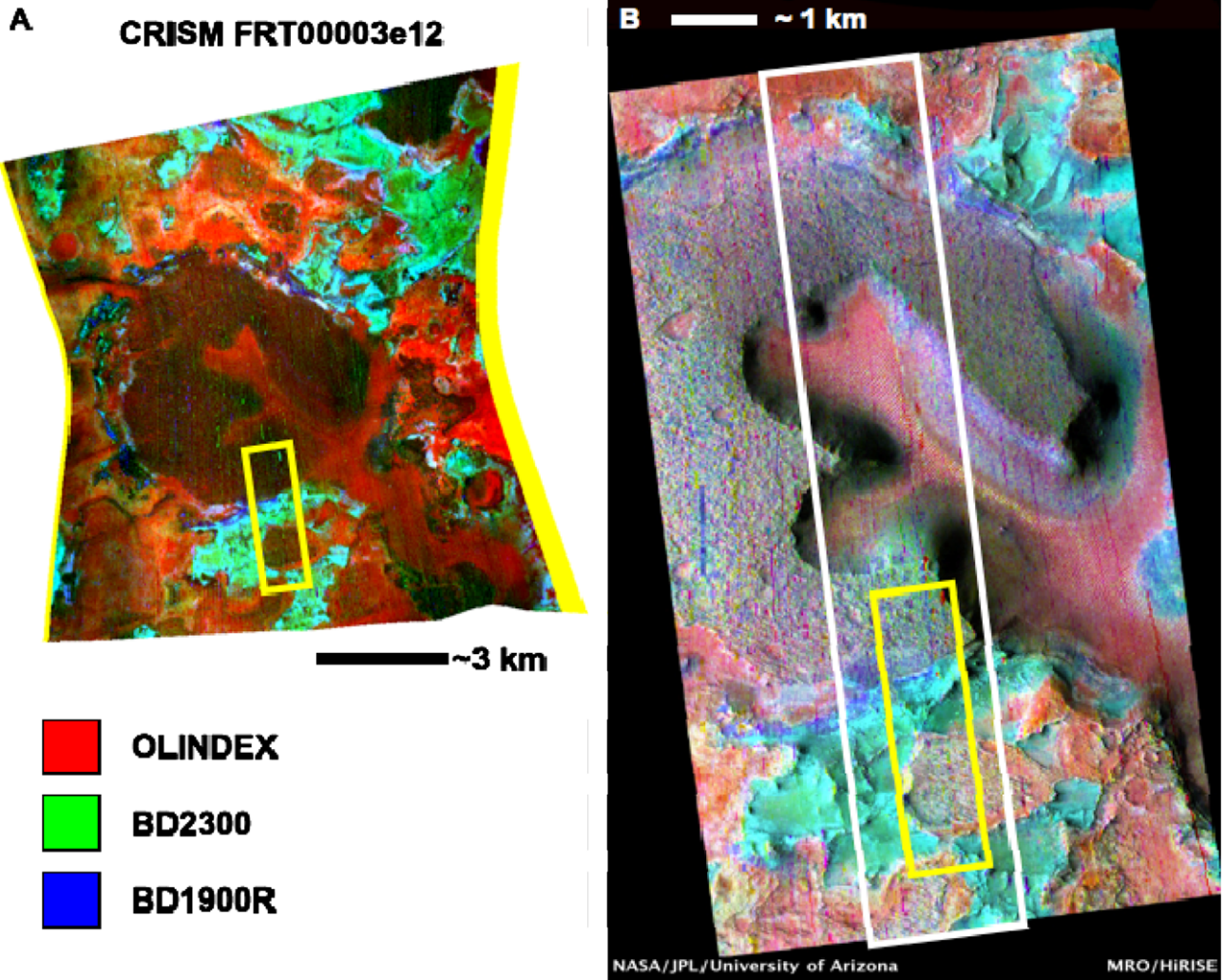
Fig. 14. Spectral mapping products based on CRISM. (A) CRISM FRT00003e12 color-composite image using the OLINDEX (red), D2300 (green), and BD1900 (blue) band parameters (see text) and (B) HSV transformed HiRISE-CRISM product using the PSP_002176_2025 red mosaic and the color information from the CRISM band parameter color-composite image. The white box outlines the extent of the HiRISE color swath and the yellow box highlights the area more closely examined in Fig. 15.

(e.g., olivine, pyroxene and in some cases calcic plagioclase cf. Fig. 15B and C). Lighter colors (yellow, orange and violet or yellow, orange and tan in Fig. 15A) are more representative of ferric bearing materials (e.g., alteration products and dust). Olivine-rich units identified by multiple spectral datasets (Hamilton and Christensen, 2005; Mustard et al., 2007; Tornabene et al., 2008), are well defined in both the HiRISE IRB and color band-ratio images (cyan

and blue, respectively). Olivine-poor basaltic materials as defined by TES and THEMIS specifically (Hamilton and Christensen, 2005; Tornabene et al., 2008) and described as "spectrally neutral" by the OMEGA and CRISM spectral datasets due to their lack of distinctive absorption features (e.g., Mustard et al., 2007, 2008) can be resolved in the HiRISE color products and are indeed distinctive from the olivine-rich variety of basaltic surface. Note that this unit

Table 4
Correlation of spectral units defined by HiRISE color products and CRISM.

Unit # Fig. 15	Unit color			Band parameter	Composition	Confirmation by other datasets
	HiRISE IRB	HiRISE band ratios	HiRISE-CRISM HSV			
1	Gray–blue	Blue and violet	Multi colored[a]	None	Basaltic	THEMIS and TES[b]
2	Yellow	Yellow	Blue	BD1900R[c]	Phyllosilicate w/weak/absent ~2.3 μm feature	OMEGA[d]
3	Orange	Yellow–orange	Cyan	BD1900R + D2300	Phyllosilicate (likely saponite/nontronite)	OMEGA[d]
4	Tan	Violet	Green	D2300	Phyllosilicate w/weak/absent bound H_2O feature	OMEGA[d]
5	Cyan	Blue	Red	OLINDEX	Olivine-rich (basaltic[e])	All

[a] Mostly Dark in CRISM band parameter color composite in Fig. 15a.
[b] Hamilton and Christensen (2005) and Tornabene et al. (2008).
[c] The "R" denotes a revised band parameter.
[d] Mangold et al. (2007) and Mustard et al. (2007).
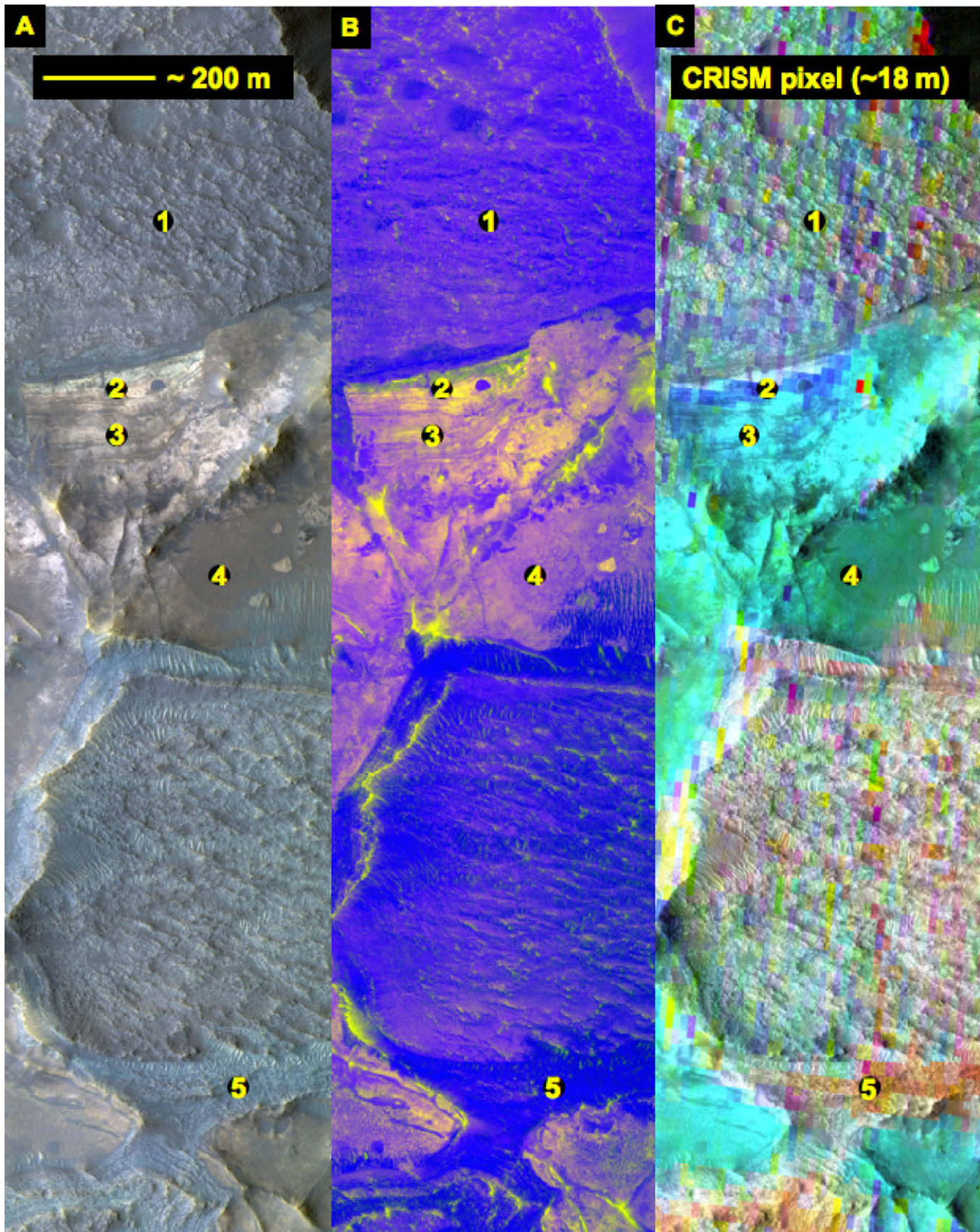[e] THEMIS and TES only (plagioclase not easily detected in VNIR).

Fig. 15. CRISM-HiRISE comparison images. Numbers refer to units outlined in Table 3. (A) A standard HiRISE color-infrared product (IRB). (B) A band-ratio image using IR/RED, IR/BG and BG/RED in R–G–B, respectively. (C) The HSV transformed HiRISE-CRISM product.

is noisy in our CRISM color composite, because none of the band parameters we chose particularly highlights the mineral composition of this unit (e.g., note the generally low DN of the "cap unit"

filling the ∼6-km crater in Fig. 14A). Materials rich in hydrous silicates can also be readily identified in the HiRISE color products, and are represented in the CRISM image by various combinations

of the D2300 and BD1900R band parameters. Areas that possess a pronounced water-bound 1.9 μm feature, but lack a strong 2.3 μm feature are yellowish in both the HiRISE IRB and color band-ratio images. Orange areas, on the other hand, possess a 2.3 μm feature, diagnostic of the Fe–Mg–OH stretching, which is green in the HSV transformed HiRISE-CRISM product. However, some small patches of yellow on the olivine-poor basaltic unit, likely, represents some martian dust. Areas that possess a 2.3 μm feature, diagnostic of the Fe–Mg–OH stretching, but lack a 1.9 μm feature can be distinguished as tan or violet in the HiRISE IRB and color band-ratio images, respectively. Areas that are likely rich in phyllosilicates (possibly saponite/nontronite), due to the presences of well-defined 2.3 and 1.9 μm features, can be distinguished by an orange coloration in both the HiRISE IRB and color band-ratio images.

The above example demonstrates the potential and utility of using HiRISE color information to extend the range of mineral and lithologic mapping from other spectral datasets to the meter scale. Combining morphologic and stratigraphic information with detailed spectral information is essential to understanding the origin of such units, and their relationship to complex geologic settings on Mars. There is little doubt combining HiRISE color with other spectral datasets will broaden our understanding and the meaning of spectral units defined by these datasets, as well as give us an appreciation of the sub-pixel mixing complexities within these datasets.

7. Conclusions

The HiRISE team has achieved a high success rate in the color processing system with few, mostly minor, artifacts. We have described here the types of products available, how they were acquired and the manner in which they were processed. The many imaging modes available allow the HiRISE operations team to acquire images that have high signal-to-noise ratios (>100) with good contrast and dynamic range. The availability of thousands of standard HiRISE color PDS products is already providing a valuable resource for the study of Mars. Consistent radiometric calibration of HiRISE color bandpasses allows comparable analysis on images taken over a range of viewing geometries and over various geological settings as well as on images taken at different times to monitor surface change. HiRISE radiometric calibration is the subject of ongoing research, and future work will include refining a procedure for atmospheric correction.

The HiRISE bandpasses are useful for distinguishing ferric- and ferrous-bearing surface materials. The use of HiRISE band ratios (presented here) is just one example of a technique that can be used to complement other higher spectral resolution datasets. However, our example image scaling algorithm requires careful cross correlation with the other Mars spectral data sets (TES, OMEGA and CRISM). HiRISE color images (both ratios and standard – IRB or RGB) are revealing mineral diversity on Mars at unprecedented spatial resolution. The addition of this high-resolution color information to multi- and hyperspectral datasets will improve mineral, lithologic and photogeologic interpretations of the martian surface.

Acknowledgments

References

Bell III, J.F., Glotch, T.D., Hamilton, V.E., McConnochiet, T., McCord, T., McEwen, A.M., Christensen, P.R., Arvidsen, R.E., 2008. Visible to near-IR multispectral orbital observations of Mars. In: Bell, J.F., III (Ed.), The Martian Surface. Composition, Mineralogy and Physical Properties. Cambridge University Press (Chapter 8).

Clark, R.N., Swayze, G.A., Gallagher, A.J., King, T.V.V., Calvin, W.M., 1993. The U.S. Geological Survey, Digital Spectral Library: Version 1: 0.2 to 3.0 microns. U.S. Geological Survey Open File Report 93-592, 1340 pp. <http://speclab.cr.usgs.gov>.

Danielson, G.E., Kupferman, P.N., Johnson, T.V., Soderblom, L.A., 1981. Radiometric performance of the Voyager cameras. J. Geophys. Res. 86, 8683–8689.

Geissler, P.E., and 12 colleagues, 2008. First in situ investigation of a dark wind streak on Mars. J. Geophys. Res. 113, E12S31.

Gillespe, A.R., Kahle, A.B., Walker, R.E., 1986. Color enhancement of highly correlated images. I. Decorrelation and HSI contrast stretches. Remote Sens. Environ. 20 (3), 209–235.

Grant, J.A., Irwin III, R.P., Grotzinger, J.P., Milliken, R.E., Tornabene, L.L., McEwen, A.S., Weitz, C.M., Squyres, S.W., Glotch, T.D., Thomson, B.J., 2008. HiRISE imaging of impact megabreccia and sub-meter aqueous strata in Holden Crater, Mars. Geology 36, 195–198.

Hamilton, V.E., Christensen, P.R., 2005. Evidence for extensive, olivine-rich bedrock on Mars. Geology 33, 433–436.

Hamilton, V.E., Christensen, P.R., McSween, H.Y., Bandfield, J.L., 2003. Searching for the source regions of Martian meteorites using MGS TES: Integrating Martian meteorites into the global distribution of igneous materials on Mars. Meteorit. Planet. Sci. 38, 871–885.

Hapke, B., 1981. Bidirectional reflectance spectroscopy 1. Theory. J. Geophys. Res. 86, 3039–3054.

Herkenhoff, K.E., Byrne, S., Russell, P.S., Fishbaugh, K.E., McEwen, A.S., 2007. Meter-scale morphology of the North Polar Region of Mars. Science 317, 1711–1715.

Hoefen, T.M., Clark, R.N., Bandfield, J.L., Smith, M.D., Pearl, J.C., Christensen, P.R., 2003. Discovery of olivine in the Nili Fossae region of Mars. Science 302, 627–630.

Keszthelyi, L., Jaeger, W., McEwen, A., Tornabene, L., Beyer, R.A., Dundas, C., Milazzo, M., 2008. High Resolution Imaging Science Experiment (HiRISE) images of volcanic terrains from the first 6 months of the Mars Reconnaissance Orbiter Primary Science Phase. J. Geophys. Res. 113, E04005.

Mangold, N., and 11 colleagues, 2007. Mineralogy of the Nili Fossae region with OMEGA/Mars Express data: 2. Aqueous alteration of the crust, J. Geophys. Res., 112, E08S04, doi:10.1029/2006JE002835.

McCord, T.B., and 11 colleagues, 2007. Mars Express High Resolution Stereo Camera spectrophotometric data: Characteristics and science analysis, J. Geophys. Res., 112, E06004, doi: 10.1029/2006JE002769.

McEwen, A.S., and 14 colleagues 2007a. Mars Reconnaissance Orbiter's High Resolution Imaging Science Experiment (HiRISE). J. Geophys. Res. 112, E05S02.

McEwen, A.S., and 32 colleagues 2007b. A closer look at water-related geologic activity on Mars. Science 317, 1706–1709.

McEwen, A.S., 60 colleagues, 2009. The High Resolution Imaging Science Experiment (HiRISE) during MRO's Primary Science Phase (PSP). Icarus 205, 2–37.

Murchie, S., and 49 colleagues 2007. Compact Reconnaissance Imaging Spectrometer for Mars (CRISM) on Mars Reconnaissance Orbiter (MRO). J. Geophys. Res. 112, E05S03.

Mustard, J.F., Poulet, F., Head, J.W., Mangold, N., Bibring, J.-P., Pelkey, S.M., Fassett, C.I., Langevin, Y., Neukum, G., 2007. Mineralogy of the Nili Fossae region with OMEGA/Mars express data: 1. Ancient impact melt in the Isidis Basin and implications for the transition from the Noachian to Hesperian. J. Geophys. Res. 112, E08S03.

Mustard, J.F., and 35 colleagues, 2008. Hydrated silicate minerals on Mars observed by the Mars Reconnaissance Orbiter CRISM instrument. Nature 454, 305–309.

Okubo, C.H., McEwen, A.S., 2007. Fracture controlled paleo-fluid flow in Candor Chasma, Mars. Science 315, 983–985.

Pelkey, S.M., and 11 colleagues, 2007. CRISM multispectral summary products: Parameterizing mineral diversity on Mars from reflectance. J. Geophys. Res. 112 (E8), E08S14.

Pieters, C.M., Englert, P.A.J., 1993. Remote Geochemical Analysis: Elemental and Mineralogical Composition. Cambridge Univ. Press (Chap. 1).

Russell, P.S., Thomas, N., Byrne, S., Herkenhoff, K., Fishbaugh, K., Okubo, C., Milazzo, M., Daubar, I., Hansen, C., McEwen, A., 2008. Seasonally-active frost-dust avalanches on a north polar scarp of Mars captured by HiRISE. Geophys. Res. Lett. 35, L23204. doi:10.1029/2008GL035790.

Soderblom, L.A., 1992. The composition and mineralogy of the martian surface from spectroscopic observations: 0.3 to 50 microns. In: Kieffer, H.H., Jakosky, B.M., Snyder, C.W., Matthews, M.S. (Eds.), Mars Tucson and London. The University of Arizona Press, pp. 557–593.

Squyres, S.W., Arvidson, R.E., and The Athena Science Team, 2008. Overview of recent results from the opportunity rover at Victoria Crater. Lunar Planet. Sci. XXXIX (1391), 2192–2193 (abstract).

Tornabene, L.L., Moersch, J.E., McSween Jr., H.Y., Hamilton, V.E., Piatek, J.L., Christensen, P.R., 2008. Surface and crater-exposed lithologic units of the Isidis Basin as mapped by coanalysis of THEMIS and TES derived data products. J. Geophys. Res. 113, E10001.

Vincent, R.K., 1997. Fundamentals of Geological and Environmental Remote Sensing. Prentice Hall, Upper Saddle River, New Jersey. 366 pp.

Weiss-Malik, M., Gorelick, N.S., Christensen, P.R., 2005. JMARS: A GIS System for Mars and Other Planets. Am. Geophys. Union (Fall Meeting) #P21C-0169 (abstract).

Weitz, C.M., Milliken, R.E., Grant, J.A., McEwen, A.S., Williams, R.M.E., Bishop, J.L., 2008. Light-toned strata and inverted channels adjacent to Juventae and Ganges chasmata, Mars. Geophys. Res. Lett. 35, L19202.

Wray, J.J., Ehlmann, B.L., Squyres, S.W., Mustard, J.F., Kirk, R.L., 2008. Compositional stratigraphy of clay-bearing layered deposits at Mawrth Vallis, Mars. Geophys. Res. Lett. 35, 12202.

Zurek, R.W., Smrekar, S.E., 2007. An overview of the Mars Reconnaissance Orbiter (MRO) science mission. J. Geophys. Res. 112, E05S01.